Chemical properties of the graptolite periderm from the Holy Cross Mountains (Central Poland)

Rafał Morga

Graptolite periderm in the Silurian shales from the Holy Cross Mountains of the Central Poland was examined by means of reflectance measurements and micro-FTIR spectroscopy. Mean graptolite reflectance (R_r) reaches 0.70–0.77%, and the vitrinite reflectance equivalent (VRE) is 0.67–0.72%. Graptolite periderm is composed predominantly of aromatic groups and rings with lesser amount of aliphatic and carbonyl/carboxyl groups. Chemical composition does not vary significantly between the samples from the two considered localities (the Prągowiec ravine and Bardo Stawy), which corresponds to the narrow range of graptolite reflectance. However, the samples from the Prągowiec ravine are characterized by higher hydrocarbon potential. It is found that many similarities occur in the chemical structure of the graptolite periderm and vitrinite within the reflectance range of $R_r \approx 0.7–1.5\%$. With increasing reflectance the length of the aliphatic chains (as inferred from the CH_2/CH_3 ratio) in the graptolite periderm decreases, and the relative content of the aromatic groups [as indicated by the $CH_{ar}/(CH_2 + CH_3)$ ratio] begins to increase at $R_r \approx 1.6\%$. This is accompanied by growth of the coherent domains and improvement in the structural order. • Key words: graptolites, chemical structure, infrared spectroscopy, Holy Cross Mountains.

Morga, R. 2020. Chemical properties of the graptolite periderm from the Holy Cross Mountains (Central Poland). *Bulletin of Geosciences 95(2)*, 205–213 (10 figures, 1 table). Czech Geological Survey, Prague. ISSN 1214-1119. Manuscript received September 6, 2019; accepted in revised form April 17, 2020; published online May 16, 2020; issued May 30, 2020.

Rafał Morga, Silesian University of Technology, Akademicka 2, 44-100 Gliwice, Poland; rafal.morga@polsl.pl

Graptolite reflectance (R_r) is one of the most important indices of thermal maturity of pre-Upper Silurian rocks, in which vitrinite does not appear (*e.g.* Goodarzi 1984, 1985; Goodarzi & Norford 1985, 1987, 1989; Link *et al*. 1990; Cole 1994; Petersen *et al*. 2013; Luo *et al*. 2020). It is commonly employed in the recognition of the unconventional hydrocarbon deposits, which frequently occur in the Cambrian–Silurian organic-rich shales (*e.g.* Więcław *et al*. 2010, Schovsbo *et al*. 2011, Jarvie 2012, Petersen *et al*. 2013). However, the chemical structure of the graptolite periderm (or fusellum *sensu* Maletz *et al*. 2014) is still not fully resolved. Periderm of living graptolites was composed of collagen-like fibrils but their corresponding fossil counterparts lack protein and they underwent the coalification process similar to plant remains (Towe & Urbanek 1972, Link *et al*. 1990). Deep insight into graptolite paleobiology was given by Maletz *et al*. (2017). Research on the chemistry of the fossilized graptolite periderm (Bustin *et al*. 1989; Suchý *et al*. 2002, 2004; Caricchi *et al*. 2016; Morga & Kamińska 2018; Luo *et al*. 2020) were mostly performed on graptolite specimens, reflectance (R_r) of which exceeded values of 0.8–1%, and still little is known about chemistry of low reflectance graptolites. The purpose of this investigation is to determine, for the first time, chemical properties of the graptolite periderms from the Holy Cross Mountains ($R_r < 0.8\%$), and compare them to those known from the previous studies. The research is a continuation of the microstructural examination performed on the same samples (Morga 2019).

Geological setting

Four samples were collected from the outcrops of the Silurian rocks in Bardo Stawy and the Prągowiec ravine in the Holy Cross Mountains (HCM), Central Poland. Both localities are situated within the Bardo Syncline – in its southern and northern limb, respectively, *ca* 35 km SEE of the town of Kielce (Fig. 1). Due to outstanding geological and paleontological importance, they are very well-described (Tomczykowa 1958, Modliński & Szymański 2001, Masiak *et al*. 2003, Trela & Salwa 2007, Smolarek *et al*. 2014, Mustafa *et al*. 2015, Schito *et al*. 2017). The Silurian rocks exhibited in Bardo Stawy belong to Llandovery series, while those in the Prągowiec ravine to Wenlock–Lower Ludlow. Two samples were taken in each locality, in the uppermost and lowermost parts of the Silurian strata, from a fresh rock to minimize the effects of weathering. Silurian rocks in Bardo Stawy

Figure 1. Geological sketch of the Holy Cross Mountains with the location of the sampling points (modified from Kremer 2001).

are mainly graptolitic dark grey shales with intercalations of radiolarian shales, while those at the Prągowiec ravine are mainly calcareous clay shales and siltstones, passing into graptolite-rich dark grey clay shales. They contain macroscopically visible graptolite remains. Geological setting and graptolite assemblages of Bardo Stawy were given in detail by Modliński & Szymański (2001), Masiak *et al*. (2003), and Trela & Salwa (2007), whereas broad description of the Prągowiec ravine geology and palaeontology one can find in Tomczykowa (1958) as well as Modliński & Szymański (2001).

Methods

Morphological and optical features of graptolites under reflected light were described in detail by Teichmüller (1978), Goodarzi (1984, 1985), Goodarzi & Norford (1985, 1987), and Link *et al*. (1990), among others.

Graptolite reflectance was measured on polished sections parallel to the bedding by the use of a Zeiss Axioskop microscope, in immersion oil (n_o = 1.518 at 23 °C) in 32 to 54 randomly chosen spots per sample. Only the well-preserved, homogenous areas were chosen. All other aspects of the measuring procedure followed the ISO 7404–5 (2009) standard. Based on that mean values (R_r) and standard deviations were calculated. All reflectance measurements were performed on non-granular graptolites (*sensu* Goodarzi 1984) to avoid possible scattering of the light beam on a granular tissue (Fig. 2).

Micro-FTIR analysis was carried out in reflectance mode, with the use of a Bio-Rad FTS-6000 spectrometer, equipped in the Bio-Rad UMA 500 microscope. Number of measurement points per sample varied between 10 and 12. Spectra were obtained within the range of 6000–750 cm^{-1}, at a resolution of 4 cm^{-1}. Interferograms were collected by co-adding of 512 scans, using a gold plate as a background. Fourier and Kramers-Krönig transformations of spectra were performed. Absorption bands were identified based on the works of Painter *et al*. (1981), Wang & Griffiths (1985), Sobkowiak & Painter (1992), Guo *et al*. (1996), Ibarra *et al*. (1996) as well as

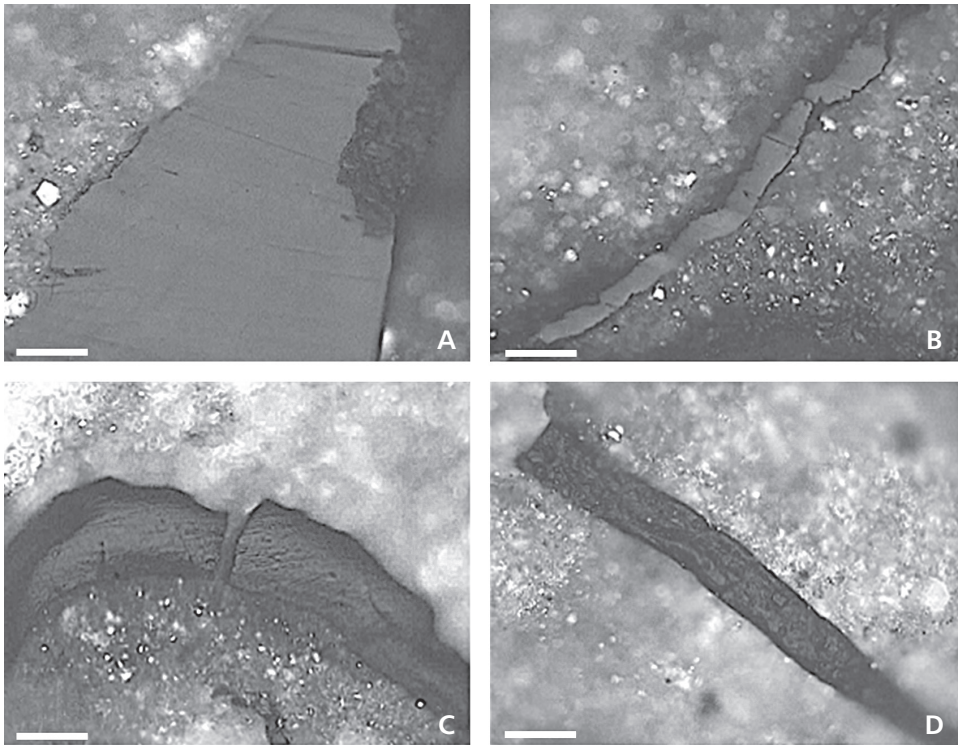

Figure 2. Microphotographs of graptolite periderm in the studied samples (section parallel to bedding, reflected light, immersion oil); A – sample P1, non-granular morphology with poorly visible lamellar structure; B – sample P2, non-granular morphology; C – sample B2, non-granular morphology; D – sample P2, granular morphology.

Bustin & Guo (1999). Curve-fitting procedure was employed regarding the aliphatic (2800–3000 cm^{-1}) and C=O + C=C (1500–1800 cm^{-1}) regions using GRAMS 32 software. The number of the bands and their initial positions were determined using the second derivative of the spectra and the data from the references (Painter *et al*. 1981; Wang & Griffiths 1985; Lin & Ritz 1993; Ibarra *et al*. 1996; Guo & Bustin 1998a, b; Geng *et al*. 2009; Chen *et al*. 2012a). Combination of Lorentzian and Gaussian curves was applied. The goodness of fit was checked by the χ^2 test. To demonstrate chemistry of the graptolite periderm the following ratios of the spectral band integration areas were used:

1) CH_{ar} (3000–3100 cm^{-1}) / [CH_2 + CH_3 (2800–3000 cm^{-1})], to show relative content of aromatic and aliphatic hydrogen functional groups *i.e*. aromaticity of the structure (Machnikowska *et al*. 2002, Lis *et al*. 2005, Chen *et al*. 2012a).
2) CH_2 (2920–2940 cm^{-1}) / CH_3 (2955–2975 cm^{-1}), related to the of the length of aliphatic chains (Wang & Griffiths 1985, Lin & Ritz 1993, Ibarra *et al*. 1996, Guo & Bustin 1998a).
3) C=O (1650–1800 cm^{-1}) / $C=C_{ar}$ (1500–1650 cm^{-1}) (Mastalerz & Bustin 1996, 1997).
4) 'A' factor, a measure of the hydrocarbon-generating potential (Ganz & Kalkreuth 1987), was determined as:

– 'A_1': [CH_2 + CH_3 (3000–2800 cm^{-1})] / [CH_2 + CH_3 (3000–2800 cm^{-1}) + C=C (1630 cm^{-1})] (Chen *et al*. 2012a, b; Wang *et al*. 2013);
– 'A_2': [CH_2 + CH_3 (3000–2800 cm^{-1})] / [CH_2 + CH_3 (3000–2800 cm^{-1}) + C=C (1500–1650 cm^{-1})] (Guo & Bustin 1998a, D'Angelo *et al*. 2010, Dutta *et al*. 2013).

5) 'C' factor, being a proxy of the maturation level (Ganz & Kalkreuth 1987), was calculated as:

– 'C_1': C=O (1710 cm^{-1}) / [C=O (1710 cm^{-1}) + C=C (1600 cm^{-1})] (Ganz & Kalkreuth 1987; Chen *et al*. 2012a, b);
– 'C_2': C=O (1650–1800 cm^{-1}) / [C=O (1650–1800 cm^{-1}) + C=C (1500–1650 cm^{-1})] (Guo & Bustin 1998a, D'Angelo *et al*. 2010, Dutta *et al*. 2013).

The 'A' and 'C' factors were determined by two methods to make it possible to compare the results with those given by different authors. Due to the presence of clay minerals, carbonates and quartz influencing the micro-FTIR spectra in the aromatic CH_{ar} out-of-plane deformation region (750–900 cm^{-1}), this band was not taken into account in calculation of the spectral ratios.

Results and discussion

Graptolite particles under reflected light show two types of morphology: non-granular (Fig. 2A–C), which predominates, and granular – rarely observed (Fig. 2D). Non-granular fragments sometimes display, poorly visible, lamellar structure, typical for the fusellar tissue (Goodarzi 1984; Goodarzi & Norford 1985, 1987; Bustin *et al*. 1989), (Fig. 2A). Granular fragments (Fig. 2D) probably compose the common canal (Goodarzi 1984; Goodarzi & Norford 1985, 1987; Bustin *et al*. 1989), which is sometimes filled with fine-grained pyrite.

The mean values of graptolite reflectance (R_r) range between 0.70% and 0.77% (s = 0.07–0.08%) (Tab. 1), indicating maturity corresponding to the oil window

Table 1. Mean reflectance (Rr), Vitrinite Reflectance Equivalent (VRE) and the selected micro-FTIR spectral parameters of the graptolite periderm.

Sample	R_r [%]	VRE [%]	$CH_{ar}/(CH_2 + CH_3)$	CH_2/CH_3	C=O/C=C	'A_1'	'A_2'	'C_1'	'C_2'
P1	0.70	0.67	0.050	2.08	0.44	0.79	0.60	0.22	0.31
n = 42	*0.07*		*0.011*	*0.28*	*0.21*	*0.09*	*0.10*	*0.11*	*0.10*
P2	0.74	0.70	0.058	1.97	0.41	0.76	0.57	0.29	0.29
n = 54	*0.08*		*0.012*	*0.18*	*0.11*	*0.09*	*0.08*	*0.12*	*0.06*
B1	0.74	0.70	0.055	2.06	0.48	0.46	0.28	0.29	0.33
n = 45	*0.07*		*0.017*	*0.31*	*0.15*	*0.15*	*0.13*	*0.11*	*0.06*
B2	0.77	0.72	0.054	1.62	0.51	0.49	0.29	0.37	0.32
n = 32	*0.07*		*0.021*	*0.15*	*0.12*	*0.18*	*0.09*	*0.15*	*0.07*

Abbreviations: Rr – mean reflectance of the graptolite periderm; VRE – Vitrinite Reflectance Equivalent; $CH_{ar}/(CH_2 + CH_3)$ – relative content of the aromatic (3000–3100 cm^{-1}) and aliphatic (2800–3000 cm^{-1}) hydrogen functional groups; CH_2/CH_3 – relative intensity of the CH_2 (2920–2940 cm^{-1}) and CH_3 (2955–2975 cm^{-1}) bands; C=O/C=C – relative content of the C=O groups (1650–1800 cm^{-1}) and C=C aromatic rings (1500–1650 cm^{-1}); 'A1' – the 'A' factor calculated as [CH_2 + CH_3 (3000–2800 cm^{-1})] / [CH_2 + CH_3 (3000–2800 cm^{-1}) + C=C (1630 cm^{-1})]; 'A2' – the 'A' factor calculated as [CH_2 + CH_3 (3000–2800 cm^{-1})] / [CH_2 + CH_3 (3000–2800 cm^{-1}) + C=C (1500 –1650 cm^{-1})]; 'C1' – the 'C' factor calculated as C=O (1710 cm^{-1}) / [C=O (1710 cm^{-1}) + C=C (1600 cm^{-1})]; 'C2' – the 'C' factor calculated as C=O (1650–1800 cm^{-1}) / [C=O (1650–1800 cm^{-1}) + C=C (1500–1650 cm^{-1})]; n – number of measurements; *italics* – the standard deviation is given.

zone. Relatively low number of measurements (32–54) is due to the limited amount of homogenous areas on the graptolite particles. The Vitrinite Reflectance Equivalent (VRE) values, calculated after Petersen *et al*. (2013), vary from 0.67% to 0.72% (Tab. 1). The results of R_r measurements conform to the data presented by Smolarek *et al*. (2014). Similar or higher values were obtained by Schito *et al*. (2017). The results are also in line with the T_{max} determinations (431–441 °C) made by Smolarek *et al*. (2014), Mustafa *et al*. (2015) and Schito *et al*. (2017). The oil window zone is also confirmed by the occurrence of scarce oil droplets, which reveal spherical shape and yellow colour under the fluorescent light.

Several bands of absorption are displayed in a typical micro-FTIR spectrum of the graptolite periderm (Fig. 3). They are assigned to OH groups (3400–3580 cm^{-1}), aromatic CH_{ar} stretching vibrations (3000–3100 cm^{-1}), and aliphatic $CH_2 + CH_3$ stretching vibrations (2800–3000 cm^{-1}). Curve-fitting procedure revealed the occurrence of six or seven bands within the aliphatic region (Fig. 4): 2985–2990 cm^{-1} – symmetric stretching vibrations of CH groups (very weak, found only in some of the spectra); 2955–2960 cm^{-1} – asymmetric stretching vibrations of CH_3 groups; 2920–2930 cm^{-1} – asymmetric stretching vibrations of CH_2 groups; 2890–2905 cm^{-1} – stretching vibrations of CH groups; 2865–2875 cm^{-1} – symmetric stretching vibrations of CH_3 groups; 2845–2855 cm^{-1} – symmetric stretching vibrations of CH_2 groups;

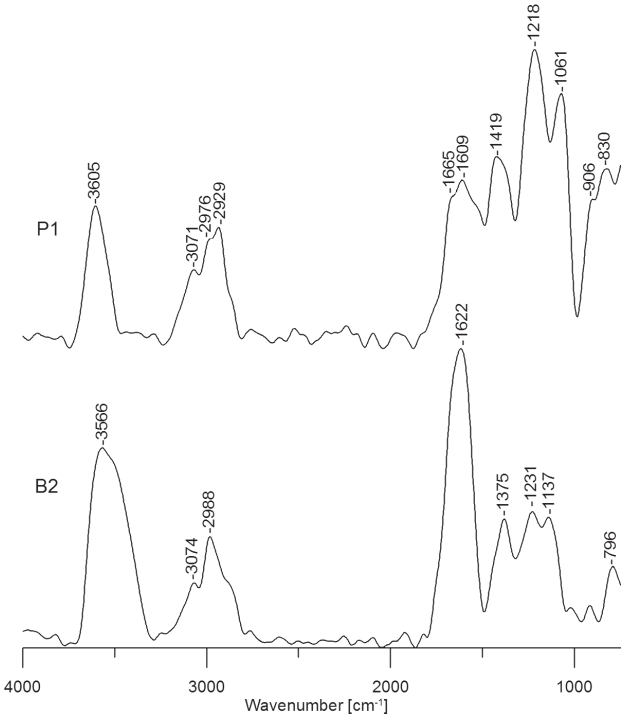

Figure 3. Representative micro-FTIR spectra of the graptolite periderm (samples P1 and B2).

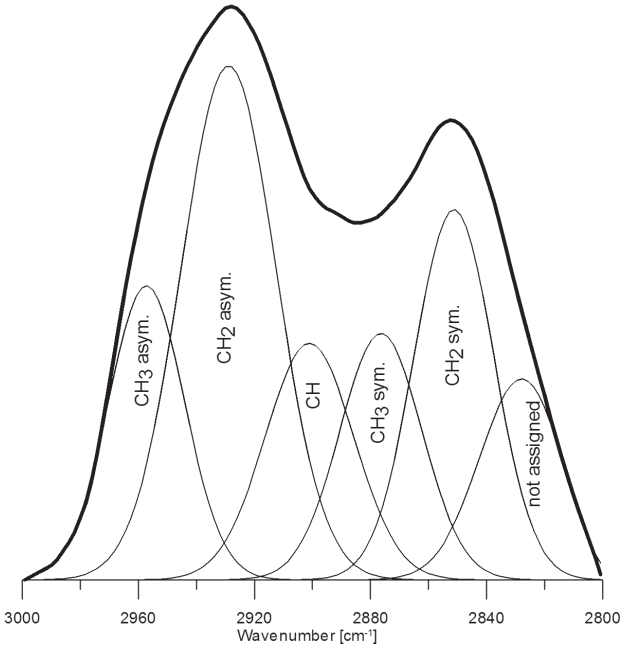

Figure 4. Curve-fitting of the aliphatic (2800–3000cm^{-1}) region for sample (sample P1).

2825–2830 cm^{-1} – a very weak band, not assigned (Ibarra *et al*. 1996).

Six bands of absorption were identified in the C=O + C=C region (1500–1800cm^{-1}) (Fig. 5): 1760–1765 cm^{-1} – C=O stretching vibrations of esters; 1710–1715 cm^{-1} – C=O stretching vibrations of carboxylic acids; 1660–1670 cm^{-1} – conjugated C=O stretching vibrations (quinones and ketones) 1615–1620 cm^{-1}, 1570–1580 cm^{-1} and 1535–1545 cm^{-1} – C=C aromatic ring stretching vibrations.

In addition, bands assigned to aliphatic $CH_2 + CH_3$ deformation (~1350–1470 cm^{-1}), aromatic ether, ester or phenolic C–O stretching vibrations (~1100–1300 cm^{-1}), aliphatic ether C–O stretching vibrations (~1030–1080 cm^{-1}), and aromatic CH_{ar} out-of-plane deformation (~750–900 cm^{-1}) are observed. Bands corresponding to clay minerals (illite, kaolinite) (~1000–1150 cm^{-1} and ~900 cm^{-1}), carbonates (mostly calcite) (~1430–1440 cm^{-1} and ~880 cm^{-1}), quartz (~1050–1100 cm^{-1} and ~780–800 cm^{-1}), as well as pyrite (~1000–1150 cm^{-1}) (Chen *et al*. 2014, 2015) are also detected.

The $CH_{ar}/(CH_2 + CH_3)$ ratio reaches 0.050–0.058 (Tab. 1, Fig. 6), being higher than the values determined for the Silurian graptolites from the Baltic Basin of Northern Poland of similar (Caricchi *et al*. 2016) or even higher reflectance (Morga & Kamińska 2018). The CH_2/CH_3 ratio decreases from 2.08 to 1.62 with the increasing reflectance, which demonstrates shortening of the aliphatic chains (Tab. 1, Fig. 7). These values correspond well with the ones determined for the Silurian graptolites

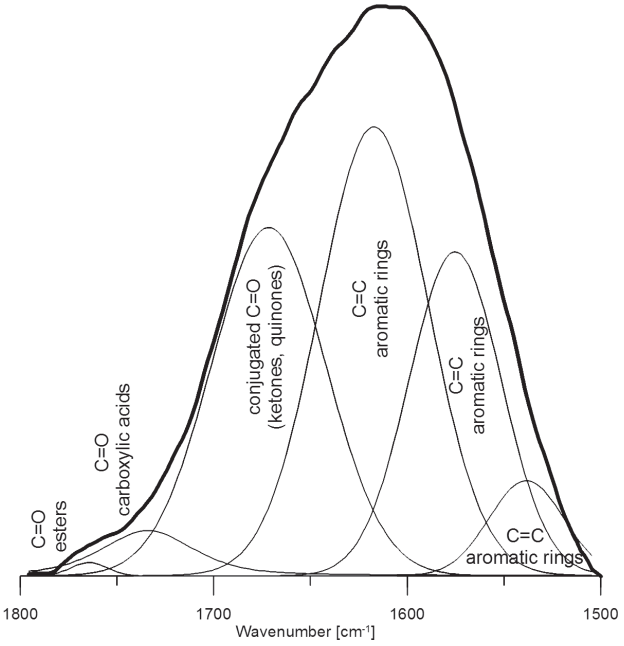

Figure 5. Curve-fitting of the C=O + C=C (1500–1800cm^{-1}) region for sample (sample B2).

(Suchý *et al*. 2002, 2004; Caricchi *et al*. 2016) as well as chitinozoans and scolecodonts (Dutta *et al*. 2013). Much lower values were observed in graptolites showing higher reflectance (Morga & Kamińska 2018). The C=O/C=C ratio is low (0.41–0.51) which reveals that weathering did not affect the chemical structure of the graptolite periderm (Tab. 1). In general, the ratio is lower in comparison to the graptolites having higher reflectance and examined from the core samples (Morga & Kamińska 2018). The 'A_1' factor varies between 0.46 and 0.79, while the 'A_2' factor between 0.28 and 0.60 (Tab. 1). Much higher values indicating higher hydrocarbon potential are observed regarding the samples from the Prągowiec ravine. Comparable results were gained for graptolites (Caricchi *et al*. 2016, Morga & Kamińska 2018), chitinozoans and scolecodonts (Dutta *et al*. 2013).

The 'C_1' factor changes from 0.22 to 0.37 and the 'C_2' factor from 0.29 to 0.33 (Tab. 1), falling within the ranges documented for the higher reflectance graptolites (Morga & Kamińska 2018), and being lower than those found by Caricchi *et al*. (2016). In general, these values are similar to those obtained for chitinozoans and scolecodonts (Dutta *et al*. 2013). Considering the 'A_2' and 'C_2' factors (Guo & Bustin 1998a, D'Angelo *et al*. 2010), the graptolite periderm represents kerogen type II or III (or can be treated as transitive type II/III) (Fig. 8), as was found in the previous studies (Bustin *et al*. 1989, Morga & Kamińska 2018).

The graptolite periderm in the studied samples is composed predominantly of aromatic groups and rings with lesser amount of aliphatic and carbonyl/carboxyl groups. The CH_2/CH_3 ratio indicates that aliphatic chains are relatively long in comparison to vitrinites and liptinites from coals (Guo & Bustin 1998a, Lin & Ritz 1993, Mastalerz & Bustin 1996, Komorek 2016, among others).

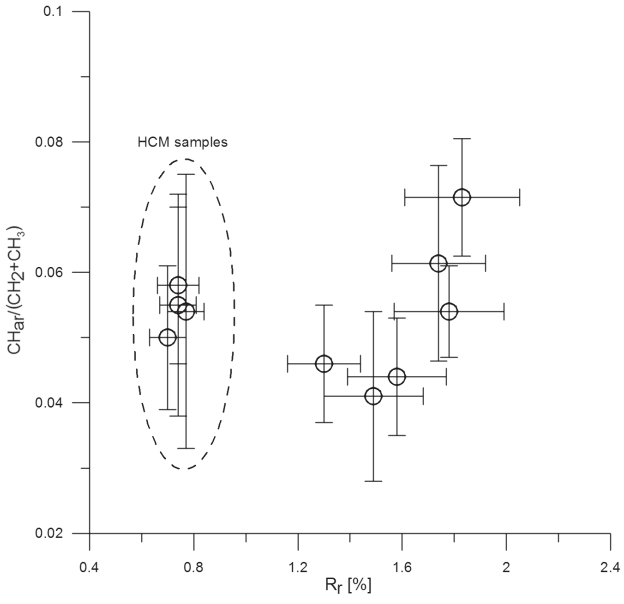

Figure 6. Relationship between the $CH_{ar}/(CH_2 + CH_3)$ ratio and the mean reflectance (R_r) of the graptolite periderm (data referring to R_r = 1.30–1.83% after Morga & Kamińska 2018).

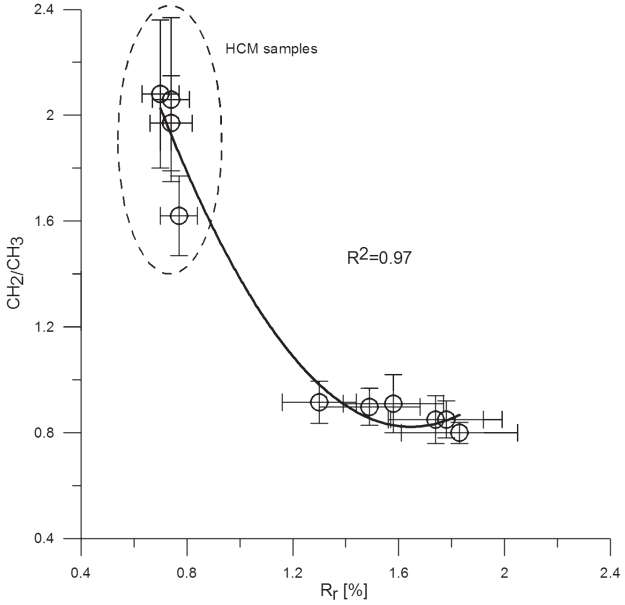

Figure 7. Relationship between the CH_2/CH_3 ratio and the mean reflectance (R_r) of the graptolite periderm (data referring to R_r = 1.30–1.83% after Morga & Kamińska 2018).

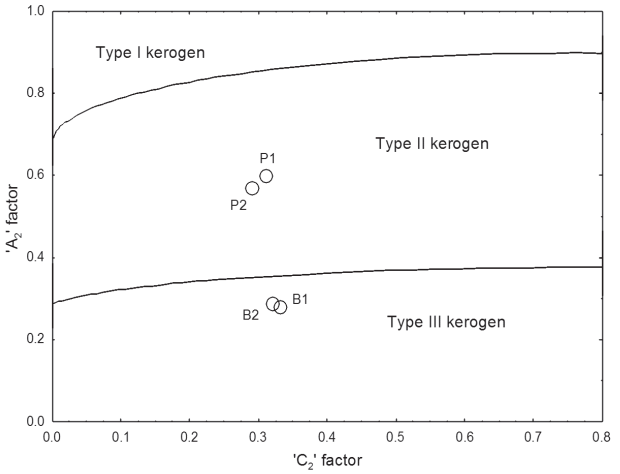

Figure 8. Kerogen type diagram of the graptolite periderm according to 'A_2' and 'C_2' factors obtained from the micro-FTIR spectra (after Guo & Bustin 1998a, D'Angelo *et al*. 2010).

The results obtained for the two analysed localities (Prągowiec ravine, Bardo Stawy) are mostly consistent. The only distinct difference is in the 'A_1' and 'A_2' factors, higher values of which indicate much higher hydrocarbon potential of shales collected in the Prągowiec ravine, even though the reflectance values are similar. It should be mentioned, however, that the 'A' factor does not show close relationship with thermal maturity indices such as R_r or T_{max}, as was revealed from shale studies (Mroczkowska-Szerszeń *et al*. 2015, Caricchi *et al*. 2016). Besides, chemical features of the graptolite periderm may not fully reflect the hydrocarbon potential of the whole rock. Furthermore, TOC content in shales occurring in both localities is very varied. It ranges from 0.3% to 2.0% for Bardo Stawy and from 0.5% to 1.2% for the Prągowiec ravine (Mustafa *et al*. 2015, Schito *et al*. 2017). This means that the values of some geochemical parameters are dependent on the place of sampling in the rock profile of the two studied localities.

Many similarities between chemical structure of the graptolite periderm and vitrinite of the adequate rank (Vitrinite Reflectance Equivalent – VRE was used for comparison) are well-established. This regards principally the $CH_{ar}/(CH_2 + CH_3)$ ratio (Machnikowska *et al*. 2002, Chen *et al.* 2012a) and the CH_2/CH_3 ratio (Lis *et al*. 2005, Petersen & Nytoft 2006, Chen *et al*. 2012a), the 'A_1' factor (Chen *et al*. 2012a). Such relation was previously suggested by Bustin *et al*. (1989) and Morga & Kamińska (2018). To some extent it is also indicated by the kerogen type of the graptolite periderm, which is frequently detected as transitive – II/III, although typical marine kerogen is of type II, and type III (represented by vitrinite) represents a terrestrial origin.

It is observed that within the whole graptolite reflectance range (R_r = 0.70–1.83%) analysed in this and previous study (Morga & Kamińska 2018) the $CH_{ar}/(CH_2 + CH_3)$ ratio stays stable and begins to increase only at higher reflectance (R_r > 1.6%), showing weak increase in aromaticity (Fig. 6). On the other hand, the CH_2/CH_3 ratio strongly decreases with increasing R_r, which reflects

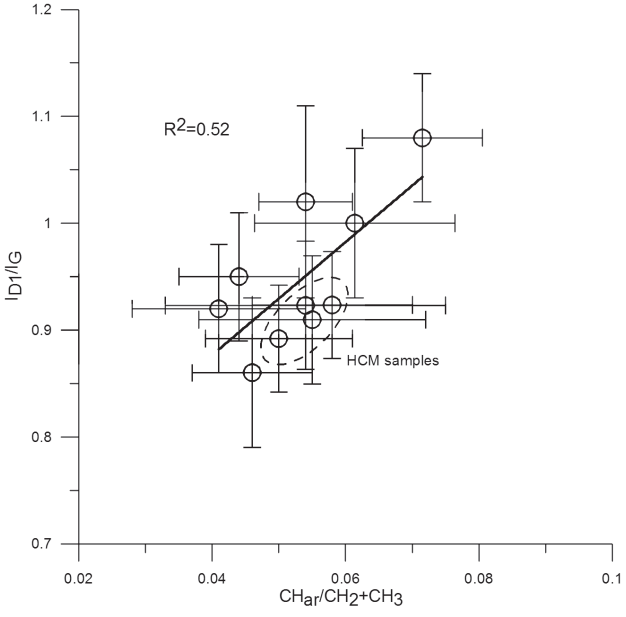

Figure 9. Relationship between the I_{D1}/I_G ratio and the the $CH_{ar}/(CH_2 + CH_3)$ ratio for the graptolite periderm (data referring to R_r = 1.30–1.83% after Morga & Kamińska 2018).

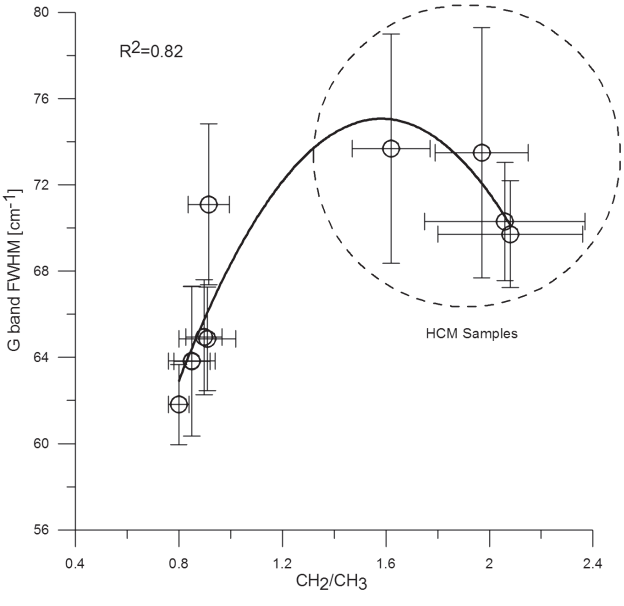

Figure 10. Relationship between the G band FWHM and the the CH_2/CH_3 ratio for the graptolite periderm (data referring to R_r = 1.30–1.83% after Morga & Kamińska 2018).

shortening of the aliphatic chains (Fig. 7). Adequate relationship was found for vitrinite (Chen *et al*. 2012a).

The microstructural examination showed that the graptolite periderm from the Holy Cross Mountains is a poorly organized carbonaceous matter (Morga 2019). The study also proved that microstructure does not vary significantly between the samples from the two considered localities. The micro-FTIR derived spectral ratios can be compared to the micro-Raman spectral parameters obtained on the same sample set (Morga & Pawlyta 2018, Morga 2019). It is seen that aromaticity of the graptolite periderm, demonstrated by the $CH_{ar}/(CH_2 + CH_3)$ ratio, tends to increase with the increasing I_{D1}/I_G ratio (Fig. 9), which is a measure of the diameter of the coherent domains (L_a) in the carbonaceous materials (Tuinstra & Koenig 1970, Ferrari & Robertson 2000 among others). The I_{D1}/I_G ratio increases with increasing L_a, when it is below 2 nm (which is the case here – see Morga & Pawlyta 2018), and decreases when L_a exceeds 2 nm (Ferrari & Robertson 2000). At $CH_2/CH_3 = 1.3$, the full width at half maximum (FWHM) of the Raman G band, which arises from the E_{2g} stretching vibrations in aromatic layers (Beyssac *et al*. 2003), begins to decrease with decreasing CH_2/CH_3 ratio (Fig. 10), which reflects improvement in the structural ordering (Kelemen & Fang 2001, Quirico *et al*. 2005). Therefore, it can be concluded that with increasing R_r the graptolite periderm (similarly to vitrinite) undergoes significant chemical and microstructural alteration. The aromaticity increases and the aliphatic chains become shorter. This is accompanied by growth of the coherent domains and increase in the structural order.

Conclusions

Graptolite periderm in the Silurian shales from the Holy Cross Mountains of Poland ($R_r = 0.70–0.77\%$; VRE = 0.67–0.72%) is composed predominantly of aromatic groups and rings with lesser amount of aliphatic and carbonyl/carboxyl groups. Chemical composition does not vary significantly between the samples from the two considered localities (the Prągowiec ravine and Bardo Stawy), which corresponds to the narrow range of graptolite reflectance. However, the samples from the Prągowiec ravine are characterized by higher hydrocarbon potential. It is found that many similarities occur in the chemical structure of the graptolite periderm and vitrinite within the reflectance range of $R_r \approx 0.7–1.5\%$. With increasing reflectance, the length of the aliphatic chains (as inferred from the CH_2/CH_3 ratio) in the graptolite periderm decreases, and the relative content of the aromatic groups [as indicated by the $CH_{ar}/(CH_2 + CH_3)$ ratio] begins to increase at $R_r \approx 1.6\%$. This is accompanied by growth of the coherent domains and improvement in the structural order.

References

Beyssac, O., Goffe, B., Petitet, J.P., Froigneux, E., Moreau, M. & Rouzaud, J.N. 2003. On the characterization of disordered and heterogenous carbonaceous materials by Raman spectroscopy. *Spectrochimica Acta Part A 59*, 2267–2276. DOI 10.1016/S1386-1425(03)00070-2

Bustin, R.M. & Guo, Y. 1999. Abrupt changes (jumps) in reflectance values and chemical compositions of artificial charcoals and inertinite in coals. *International Journal of Coal Geology 38*, 237–260. DOI 10.1016/S0166-5162(98)00025-1

Bustin, R.M., Link, C. & Goodarzi, F. 1989. Optical properties and chemistry of graptolite periderms following laboratory simulated maturation. *Organic Geochemistry 14*, 355–364. DOI 10.1016/0146-6380(89)90001-6

Caricchi, C., Corrado, S., Di Paolo, L., Aldega, L. & Grigo, D. 2016. Thermal maturity of Silurian deposits in the Baltic Syneclise (on-shore Polish Baltic Basin): contribution to unconventional resources assessment. *Italian Journal of Geosciences 135*, 383–393. DOI 10.3301/IJG.2015.16

Chen, Y., Mastalerz, M. & Schimmmelmann, A. 2012a. Characterization of chemical functional groups in macerals across different coal ranks via micro-FTIR spectroscopy. *International Journal of Coal Geology 104*, 22–33. DOI 10.1016/j.coal.2012.09.001

Chen, Y., Caro, L.D., Mastalerz, M., Schimmmelmann, A. & Blandon, A. 2012b. Mapping the chemistry of resinite, funginite and associated vitrinite in coal with micro-FTIR. *Journal of Microscopy 249*, 69–81. DOI 10.1111/j.1365-2818.2012.03685.x

Chen, Y., Furmann, A., Mastalerz, M. & Schimmmelmann, A. 2014. Quantitative analysis of shales by KBr-FTIR and micro-FTIR. *Fuel 116*, 538–549. DOI 10.1016/j.fuel.2013.08.052

Chen, Y., Zou, C., Mastalerz, M., Hu, S., Gasaway, C. & Tao, X. 2015. Applications of Micro-Fourier Transform Infrared Spectroscopy (FTIR) in the Geological Sciences—A Review. *International Journal of Molecular Sciences 16*, 30223–30250. DOI 10.3390/ijms161226227

Cole, G.A. 1994. Graptolite–chitinozoan reflectance and its relationship to other geochemical maturity indicators in the Silurian Qusaiba Shale, Saudi Arabia. *Energy & Fuels 8*, 1443–1459. DOI 10.1021/ef00048a035

D'Angelo, J., Zodrow, E. & Camargo, A. 2010. Chemometric study of functional groups in Pennsylvanian gymnosperm plant organs (Sydney Coalfield, Canada): Implications for chemotaxonomy and assessment of kerogen formation. *Organic Geochemistry 41*, 1312–1325. DOI 10.1016/j.orggeochem.2010.09.010

Dutta, S., Hartkopf-Fröder, C., Witte, K., Brocke, R. & Mann, U. 2013. Molecular characterization of fossil palynomorphs by transmission micro-FTIR spectroscopy: Implications for hydrocarbon source evaluation. *International Journal of Coal Geology 115*, 13–23. DOI 10.1016/j.coal.2013.04.003

Ferrari, A.C. & Robertson, J. 2000. Interpretation of Raman spectra of disordered and amorphous carbon. *Physical Review B 61*, 14095–14107. DOI 10.1103/PhysRevB.61.14095

Ganz, H. & Kalkreuth, W. 1987. Application of infrared spectroscopy to the classification of kerogen-types and the evaluation of source rock and oil shale potentials. *Fuel 66*, 708–711. DOI 10.1016/0016-2361(87)90285-7

Geng, W., Nakajima, T., Takanashi, H. & Ohki, A. 2009. Analysis of carboxyl group in coal and coal aromaticity by Fourier transform infrared (FT-IR) spectrometry. *Fuel 88*, 139–144. DOI 10.1016/j.fuel.2008.07.027

Goodarzi, F. 1984. Organic petrography of graptolite fragments from Turkey. *Marine and Petroleum Geology 1*, 202–210. DOI 10.1016/0264-8172(84)90146-6

Goodarzi, F. 1985. Dispersion of optical properties of graptolite periderms with increased maturity in early Paleozoic sediments. *Fuel 64*, 1735–1740. DOI 10.1016/0016-2361(85)90401-6

Goodarzi, F. & Norford, B.S. 1985. Graptolites as indicator of the temperature histories of rocks. *Journal of Geological Society London 142*, 1089–1099. DOI 10.1144/gsjgs.142.6.1089

Goodarzi, F. & Norford, B.S. 1987. Optical properties of graptolite periderm – a review. *Bulletin of Geological Society Denmark 35*, 141–147.

Goodarzi, F. & Norford, B.S. 1989. Variation of graptolite reflectance with depth of burial. *International Journal of Coal Geology 11*, 127–141. DOI 10.1016/0166-5162(89)90002-5

Guo, Y. & Bustin, R.M. 1998a. Micro-FTIR spectroscopy of liptinite macerals in coal. *International Journal of Coal Geology 36*, 259–275. DOI 10.1016/S0166-5162(97)00044-X

Guo, Y. & Bustin, R.M. 1998b. FTIR spectroscopy and reflectance of modern charcoals and fungal decayed woods: implications for studies of inertinite in coals. *International Journal of Coal Geology 37*, 29–53. DOI 10.1016/S0166-5162(98)00019-6

Guo, Y., Renton, J.J. & Penn, J.H. 1996. FTIR microspectroscopy of particular liptinite- (lopinite-) rich, Late Permian coals from Southern China. *International Journal of Coal Geology 29*, 187–197. DOI 10.1016/0166-5162(95)00024-0

Ibarra, J.V., Munoz, E. & Moliner, R. 1996. FTIR study of the evolution of coal structure during the coalification process. *Organic Geochemistry 24*, 725–735. DOI 10.1016/0146-6380(96)00063-0

ISO 7404–5 2009. *Methods for the Petrographic Analysis of Coals – Part 5: Method of Determining Microscopically the Reflectance of Vitrinite*. International Organization for Standardization.

Jarvie, D.M. 2012. Shale resource systems for oil and gas: part 1 – shale–gas resource systems. *American Association of Petroleum Geologists Memoir 97*, 69–87.

Kelemen, S.R. & Fang, H.R. 2001. Maturity trends in Raman spectra from kerogen and coals. *Energy & Fuels 14*, 653–658. DOI 10.1021/ef0002039

Komorek, J. 2016. Internal structure of vitrinite and sporinite in the view of micro-FTIR spectroscopy using the example of coal from the seam 405 (USCB). *Archives of Mining Sciences 61*, 729–748. DOI 10.1515/amsc-2016-0050

Kremer, B. 2001. Acritarchs from the Upper Ordovician of southern Holy Cross Mountains, Poland. *Acta Palaeontologica Polonica 46*, 595–601.

Lin, R. & Ritz, P. 1993. Studying the chemistry of individual macerals using IR microspectroscopy, and the structural implications on oil vs. gas/condensate proneness and 'low-rank' generation. *Organic Geochemistry 20*, 695–706. DOI 10.1016/0146-6380(93)90055-G

Link, C.M., Bustin, R.M. & Goodarzi, F. 1990. Petrology of graptolites and their utility as indices of thermal maturity in Lower Paleozoic strata in northern Yukon, Canada. *International Journal of Coal Geology 15*, 113–135. DOI 10.1016/0166-5162(90)90007-L

Lis, G.P., Mastalerz, M., Schimmmelmann, A., Lewan, M.D. & Stankiewicz, B.A. 2005. FTIR absorption indices for thermal maturity in comparison with vitrinite reflectance R_o in type-II kerogens from Devonian black shales. *Organic Geochemistry 36*, 1533–1552. DOI 10.1016/j.orggeochem.2005.07.001

Luo, Q., Goodarzi, F., Zhong, N., Wang, Y., Qiu, N., Skovsted, C.B., Suchý, V., Schovsbo, N.H., Morga, R., Xu, Y., Hao, J., Liu, A., Wu, J., Cao, W. , Min, X. & Wu, J. 2020. Graptolites as fossil geo-thermometers and source material of hydrocarbons: An overview of four decades of progress. *Earth-Science Reviews 200*, art. 103000. DOI 10.1016/j.earscirev.2019.103000

Machnikowska, H., Krztoń, A. & Machnikowski, J. 2002. The characterization of coal macerals by diffuse reflectance infrared spectroscopy. *Fuel 81*, 245–252. DOI 10.1016/S0016-2361(01)00125-9

Maletz, J. 2017. *Graptolite Paleobiology*. *Topics in Palaeobiology*. 323 pp. Wiley-Blackwell. DOI 10.1002/9781118515624

Maletz, J., Bates, D.E.B., Brussa, E.D., Cooper, R.A., Lenz, A.C., Riva, J.F., Toro, B.A. & Zhang, Y.D. 2014. Treatise on Invertebrate Paleontology, Part V, revised. Chapter 12: Glossary of the Hemichordata. *Treatise Online 62*, 1–23. DOI 10.17161/to.v0i0.4710

Masiak, M., Podhalańska, T. & Stempień-Sałek, M. 2003. Ordovician-Silurian boundary in the Bardo Syncline, Holy Cross Mountains, Poland – new data on fossil assemblages and sedimentary succession. *Geological Quarterly 47*, 311–330.

Mastalerz, M. & Bustin, R.M. 1996. Application of reflectance micro-Fourier Transform infrared analysis to the study of coal macerals: an example from the Late Jurassic to Early Cretaceous coals of the Mist Mountain Formation, British Columbia, Canada. *International Journal of Coal Geology 32*, 55–67. DOI 10.1016/S0166-5162(96)00030-4

Mastalerz, M. & Bustin, R.M. 1997. Variation in the chemistry of macerals in coals of the Mist Mountain Formation, Elk Valley coalfield, British Columbia, Canada. *International Journal of Coal Geology 33*, 43–59. DOI 10.1016/S0166-5162(96)00003-1

Modliński, Z. & Szymański, B. 2001. The Silurian of the Nida, Holy Cross Mts. and Radom areas, Poland – a review. *Geological Quarterly 45*, 435–454.

Morga, R. 2019. About the microstructure of the graptolite periderm – examples from the Holy Cross Mountains (Poland).

IOP Conference Series: Earth and Environmental Sciences 362, art. 012076. DOI 10.1088/1755-1315/362/1/012076

Morga, R. & Kamińska, M. 2018. The chemical composition of graptolite periderm in the gas shales from the Baltic Basin of Poland. *International Journal of Coal Geology 199*, 10–18. DOI 10.1016/j.coal.2018.09.016

Morga, R. & Pawlyta, M. 2018. Microstructure of graptolite periderm in Silurian gas shales of Northern Poland. *International Journal of Coal Geology 189*, 1–7. DOI 10.1016/j.coal.2018.02.012

Mroczkowska-Szerszeń, M., Ziemianin, K., Brzuszek, P., Matyasik, I. & Jankowski, L. 2015. The organic matter type in the shale rock samples assessed by FTIR-ATR analyses. *Nafta-Gaz 71*, 361–369.

Mustafa, K., Sephton, M., Watson, J., Spathopoulos, F. & Krzywiec, P. 2015. Organic geochemical characteristics of black shales across the Ordovician-Silurian boundary in the Holy Cross Mountains, central Poland. *Marine and Petroleum Geology 66*, 1042–1055. DOI 10.1016/j.marpetgeo.2015.08.018

Painter, P.C., Snyder, R.W., Starsinic, M., Coleman, M.M., Kuehn, D.W. & Davis, A. 1981. Concerning the application of FT-IR to the study of coal: A critical assessment of band assignments and the application of spectral analysis programs. *Applied Spectroscopy 35*, 475–485. DOI 10.1366/0003702814732256

Petersen, H.I. & Nytoft, H.P. 2006. Oil generation capacity of coals as a function of coal age and aliphatic structure. *Organic Geochemistry 37*, 558–583. DOI 10.1016/j.orggeochem.2005.12.012

Petersen, H.I., Schovsbo, N.H. & Nielsen A.T. 2013. Reflectance measurements of zooclasts and solid bitumen in Lower Paleozoic shales, southern Scandinavia: Correlation to vitrinite reflectance. *International Journal of Coal Geology 114*, 1–18. DOI 10.1016/j.coal.2013.03.013

Quirico, E., Rouzaud, J.-N., Bonal, L. & Montagnac, G. 2005. Maturation grade of coals as revealed by Raman spectroscopy: Progress and problems. *Spectrochimica Acta Part A 61*, 2368–2377. DOI 10.1016/j.saa.2005.02.015

Schito, A., Corrado, S., Trolese, M., Aldega, L., Caricchi, C., Cirilli, S., Grigo, D., Guedes, A., Romano, C., Spina, A. & Valentim, B. 2017. Assessment of thermal evolution of Paleozoic successions of the Holy Cross Mountains (Poland). *Marine and Petroleum Geology 80*, 112–132. DOI 10.1016/j.marpetgeo.2016.11.016

Schovsbo, N.H., Nielsen, A.T., Klitten, K., Mathiesen, A. & Rasmussen, P. 2011. Shale gas investigations in Denmark: Lower Palaeozoic shales on Bornholm. *Geological Survey of Denmark and Greenland Bulletin 23*, 9–14.

Smolarek, J., Marynowski, L., Spunda, K. & Trela, W. 2014. Vitrinite equivalent reflectance of Silurian black shales from the Holy Cross Mountains, Poland. *Mineralogia 45*, 79–96. DOI 10.1515/mipo-2015-0006

Sobkowiak, M. & Painter, P. 1992. Determination of the aliphatic and aromatic CH contents of coals by FT-i.r.: studies of coal extracts. *Fuel 71*, 1105–1125. DOI 10.1016/0016-2361(92)90092-3

Suchý, V., Šafanda, J., Sýkorová, I., Stejskal, M., Machovič, V. & Melka, K. 2004. Contact metamorphism of Silurian black shales by a basalt sill: geological evidence and thermal modelling in the Barrandian Basin. *Bulletin of Geosciences 79*, 133–147.

Suchý, V., Sýkorová, I., Stejskal, M., Šafanda, J., Machovič, V. & Novotná, M. 2002. Dispersed organic matter from Silurian shales of the Barrandian Basin, Czech Republic: optical properties, chemical composition and thermal maturity. *International Journal of Coal Geology 53*, 1–25. DOI 10.1016/S0166-5162(02)00137-4

Teichmüller M. 1978. Nachweis von Graptolithen – Periderm in geschieferten Gesteinen mit Hilfe kohlenpetrologischer Methoden. *Neues Jahrbuch für Geologie und Paläontologie, Monatshefte 7*, 430–447.

Tomczykowa, E 1958. Fauna z łupków graptolitowych syluru niecki bardziańskiei Gór Świętokrzyskich. *Geological Quarterly 2*, 321–346.

Towe, K.M. & Urbanek, A. 1972. Collagen-like structure in Ordovician graptolite periderm. *Nature 237*, 443–445. DOI 10.1038/237443a0

Trela, W. & Salwa, S. 2007. Lithostratigraphy of the Lower Silurian in Bardo Stawy (southern Holy Cross Mountains): relation to sea level change and oceanographic circulation. *Przegląd Geologiczny 55*, 971–978.

Tuinstra, F. & Koenig, J.L. 1970. Raman spectrum of graphite. *Journal Chemical Physics 53*, 1126–1130. DOI 10.1063/1.1674108

Wang, S.H. & Griffiths, P.R. 1985. Resolution enhancement of diffuse reflectance IR spectra of coals by Fourier self-deconvolution, 1, C–H stretching and bending modes. *Fuel 64*, 229–236. DOI 10.1016/0016-2361(85)90223-6

Wang, S., Tang, Y., Schobert, H., Jiang, D., Guo, X., Huang, F., Guo, Y. & Su, Y. 2013. Chemical compositional and structural characteristics of Late Permian bark coals from Southern China. *Fuel 126*, 116–121. DOI 10.1016/j.fuel.2014.02.026

Więcław, D., Kotarba, M., Kosakowski, P., Kowalski, A. & Grotek, I. 2010. Habitat and hydrocarbon potential of the lower Paleozoic source rocks in the Polish part of the Baltic region. *Geological Quarterly 54*, 159–182.